

## Measurement of the 3D Born-Oppenheimer Potential of a Proton in a Hydrogen-Bonded System via Deep Inelastic Neutron Scattering: The Superprotonic Conductor $\text{Rb}_3\text{H}(\text{SO}_4)_2$

D. Homouz,<sup>1</sup> G. Reiter,<sup>1</sup> J. Eckert,<sup>2</sup> J. Mayers,<sup>3</sup> and R. Blinc<sup>4</sup>

<sup>1</sup>Physics Department, University of Houston, Houston, Texas, 77204 USA

<sup>2</sup>LANSCE, Los Alamos National Laboratory, and University of California, Santa Barbara, California, USA

<sup>3</sup>ISIS, Rutherford Appelton Laboratory, Chilton, Didcot, England, United Kingdom

<sup>4</sup>Stefan Jozef Institut, Ljubljana, Slovenia

(Received 11 November 2006; published 14 March 2007)

We report the first direct measurement of the proton 3-D Born-Oppenheimer potential in any material. The proton potential surfaces in the hydrogen-bonded superprotonic conductor  $\text{Rb}_3\text{H}(\text{SO}_4)_2$  are extracted from the momentum distribution measured using Deep Inelastic Neutron Scattering (DINS). The potential has a single minimum along the bond direction, which accounts for the absence of the antiferroelectric transition seen in the deuterated material. The measured potential is in qualitative agreement with phenomenological double Morse potentials that have been used to describe hydrogen bonds in other systems.

DOI: 10.1103/PhysRevLett.98.115502

PACS numbers: 61.18.-j

The shape of the Born-Oppenheimer (BO) potential of the proton in hydrogen-bonded systems plays an essential role in a variety of phase transitions and in proton conductivity in biologically and technically important materials. We present here the first direct, model independent measurement of the 3-D proton BO potential in any system, and, in particular, in a hydrogen-bonded system of technological interest,  $\text{Rb}_3\text{H}(\text{SO}_4)_2$  [1]. These measurements can be used to investigate the accuracy of *ab initio* calculations and provide a data base for their improvement, to interpret neutron and light scattering measurements, and as input to simulations of the dynamics of the system containing the bond. In this case, the material is a superprotonic conductor, and the form of the potential is essential information in simulating the transport of the protons. The measurement agrees qualitatively with earlier phenomenological attempts to characterize the O-H-O bond using empirical Morse potentials [2]. A previous determination of the potential by means of inelastic neutron scattering and Raman scattering in the system we have measured [3] is qualitatively wrong.

We extract the information needed to determine the potential from a measurement of the proton momentum distribution by a procedure suggested by Reiter and Silver [4]. In order to do this, the proton must be at a center of inversion symmetry, the interaction with other protons must be negligible, and the temperature must be lower than any excitations of the proton vibrations. All of these conditions can be satisfied in  $\text{Rb}_3\text{H}(\text{SO}_4)_2$ , which is of interest both as a superprotonic conductor at high temperatures and because of the large isotope effect it exhibits at low temperatures. The deuterated material has an antiferroelectric phase transition at 82 K, while the protonated version has no antiferroelectric transition at all [5]. An earlier experiment on  $\text{KH}_2\text{PO}_4$  (KDP) [6] was able to extract the potential along the bond, but it was necessary to assume that the potential was separable because of the

insufficient quality of the data. We make no assumptions here about the *a priori* form of the potential.

The geometry of this H-bonded system consists of pairs of sulphate tetrahedra hydrogen bonded together, well separated from other pairs. The distance between nearest neighbor protons is 5.07 Å, leaving the protons on different bonds effectively isolated from each other. The  $A2/a$  space group places the average proton position at a center of inversion. This allows us to assume that the ground state momentum wave function is real. We will argue later that this is not just a statistical average and that the hydrogen bond is itself symmetric.

Several experimental studies suggested the presence of a double well proton potential along the hydrogen bond [3,7,8] at same time that other experimental studies as well as theoretical calculations supported single well potential models [2,9,10]. We find that the potential is unambiguously a single well along the bond. Fillaux *et al.*'s [3] potential is far too broad to be able to describe our momentum distribution measurements.

The momentum distribution is measured with Deep Inelastic Neutron Scattering (DINS), also called Neutron Compton Scattering (NCS). DINS is inelastic neutron scattering in the limit of high momentum transfer  $\vec{q}(30\text{--}100 \text{ \AA}^{-1})$ . In this limit, the impulse approximation [4] can be used to interpret the scattering process which means that neutrons scatter from individual protons in the same manner that freely moving particles scatter from each other. Thus the scattering function depends only on the proton momentum distribution  $n(\vec{p})$ . In the impulse approximation limit, the neutron scattering function is related to the momentum distribution  $n(\vec{p})$  by the relation

$$S(\vec{q}, \omega) = \frac{M}{q} \int n(\vec{p}) \delta(y - \hat{q} \cdot \vec{p}) d\vec{p} = \frac{M}{q} J(\hat{q}, y) \quad (1)$$

where  $y = \omega - q^2/2M$ .  $S(\vec{q}, \omega)$  is the Radon transform of

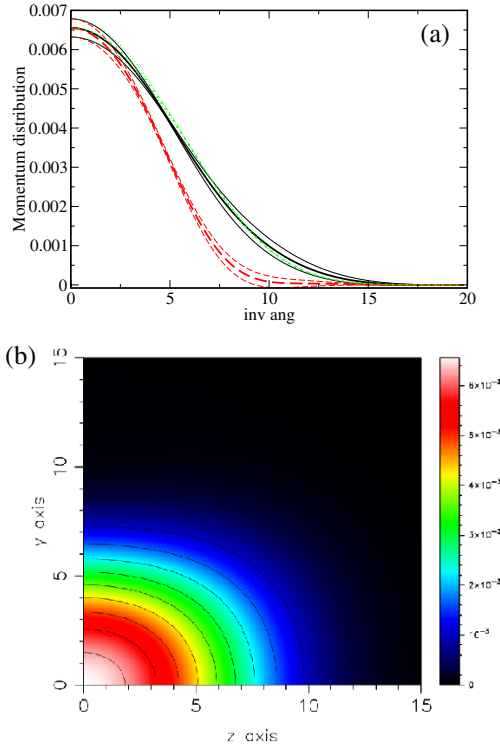


FIG. 1 (color online). Proton momentum distribution for  $\text{Rb}_3\text{H}(\text{SO}_4)_2$  at 10 K: (a) along the  $x$ -axis (solid line),  $y$ -axis (dashed line), and  $z$ -axis (dotted line), the rms errors are shown in dashed lines, (b) in the  $yz$  plane.

$n(\vec{p})$ . The relation is invertible by a series expansion method [4,11] that represents  $n(\vec{p})$  in terms of three parameters  $\sigma_i$ , giving the Gaussian widths in three directions, and a set of anharmonic parameters,  $a_{n,l,m}$ , giving the deviations from an anisotropic Gaussian distribution.

For temperatures that are well below the lowest possible excitation energy of the proton,  $n(\vec{p})$  is determined almost entirely by the ground state of the proton, as will be the case with our measurements. The shape of  $n(\vec{p})$  is determined by the BO potential that localizes the proton.

Using a single particle potential to interpret DINS measurements allows us to relate  $n(\vec{p})$  directly to the proton ground state wave function via

$$n(\vec{p}) = \frac{1}{(2\pi\hbar)^3} \left| \int \psi(\vec{r}) \exp(i\vec{p} \cdot \vec{r}) d\vec{r} \right|^2. \quad (2)$$

We can take the momentum wave function to be real if the bond is symmetric. This allows us to calculate the spatial wave function as well as the BO potential. This is given from the one-particle Schroedinger equation by

$$E - V(\vec{r}) = \frac{\int \exp(i\vec{p} \cdot \vec{r}) \frac{p^2}{2m} \sqrt{n(\vec{p})} d\vec{p}}{\int \exp(i\vec{p} \cdot \vec{r}) \sqrt{n(\vec{p})} d\vec{p}}. \quad (3)$$

The DINS experiments were performed on the VESUVIO instrument at ISIS [12]. Measurements were done on single crystal samples of  $\text{Rb}_3\text{H}(\text{SO}_4)_2$  at 10 and 70 K. The  $z$  axis is chosen along the bond, the  $y$  axis along

the line joining the two Rb atoms in the  $ab$  plane. Two planes of data are collected for the crystal sample. One plane is the  $ab$  plane where  $b$  is the unique axis of the monoclinic crystal. The other plane is the  $ac^*$ , where the  $c^*$  axis is perpendicular to the  $ab$  plane. The unit cell for  $\text{Rb}_3\text{H}(\text{SO}_4)_2$  has 2 H bonds at  $60^\circ$  from each other. The momentum distribution of each bond is represented as in Refs. [6,11] and the contribution of both bonds added to fit the data. The measurements were done with 30 detectors in a plane, distributed with scattering angles from  $32^\circ$  to  $68^\circ$ .

The fitting parameters for the momentum distribution at the two temperatures are given in Table I. There is no phase transition in the protonated  $\text{Rb}_3\text{H}(\text{SO}_4)_2$  for temperatures below 70 K. Yet the values of these parameters are accurate enough to reveal some structural changes between 10 and 70 K, due simply to the expansion of the crystal. The proton momentum distribution along the three axes is shown in Fig 1(a). Its projection in the  $yz$  plane is shown in Fig. 1(b). These figures show no sign of proton coherence over two sites, which would show up as an oscillation in the momentum distribution [6]. This can be also seen from the BO potential surface plot in the same plane Fig. 2. Along the bond direction,  $z$ -axis, the potential at both temperatures has a single well with a flat bottom. This is shown more clearly in Fig. 2(a) where we show the potential in all three coordinate directions, along with the errors [11] in the measurement. In general, the measurement can only be done out to distances for which the proton has some significant probability of penetrating. For our present statistics, this is about 2.5 standard deviations of the spatial wave function in the direction of interest.

Although there is no double well along the bond, it is clear that there is an off axis barrier to motion out of the well into the next well. The barrier height is about 350 meV, approximately half the value that was inferred from NMR measurements on the deuterated material [7] at temperatures above room temperature. In Fig. 3(a), we compare this potential with the double-well model sug-

TABLE I. The harmonic scale factors and the anharmonic fitting coefficients and their variances for the momentum distribution measured at 10 and 70 K.

	Harmonic Coefficients			
	10 K	70 K		
$\sigma_z$ ( $\text{\AA}^{-1}$ )	4.60	4.70		
$\sigma_x$ ( $\text{\AA}^{-1}$ )	4.35	4.36		
$\sigma_y$ ( $\text{\AA}^{-1}$ )	3.73	3.65		
Anharmonic Coefficients				
	10 K	70 K		
$nlm$	$a_{nlm}$	$\delta a_{nlm}$	$a_{nlm}$	$\delta a_{nlm}$
4 0 0	$-2.05 \times 10^{-1}$	$2.0 \times 10^{-2}$	$-1.91 \times 10^{-1}$	$2.0 \times 10^{-2}$
4 4 2	$-8.76 \times 10^{-2}$	$4.0 \times 10^{-2}$	$-1.02 \times 10^{-1}$	$4.0 \times 10^{-2}$
4 4 4	$-8.09 \times 10^{-2}$	$1.0 \times 10^{-2}$	$-1.26 \times 10^{-1}$	$1.0 \times 10^{-2}$
6 6 6	0.0		$-2.52 \times 10^{-2}$	$1.0 \times 10^{-2}$
10 6 6	$1.49 \times 10^{-3}$	$9.0 \times 10^{-4}$	$2.38 \times 10^{-3}$	$1.01 \times 10^{-3}$
10 8 8	$-3.92 \times 10^{-3}$	$3.0 \times 10^{-3}$	$-9.48 \times 10^{-3}$	$2.0 \times 10^{-3}$

gested by Fillaux *et al.* [3] to interpret the INS measurements for the vibrational spectrum of  $\text{Rb}_3\text{H}(\text{SO}_4)_2$  at 20 K. This model is supposed to produce energy levels that can be assigned to the peaks in the INS spectrum. Calculating the momentum distribution for Fillaux *et al.*'s model and comparing it with our measurement along the bond direction, Fig. 3(b) shows that the inferred potential is in fact far from anything that could reproduce our measured momentum distribution. Ignoring the motion of the heavy ions, and calculating the excitation energies from the measured potential, we find that the first three excitations are at 125, 147, and 155 meV. There are only two strong peaks identifiable in the INS spectrum, at 142 and 192 meV. Fillaux *et al.* assigned these to the transverse modes and identified a band at around 50 meV as the result of the 0–2 transition along the bond interacting with the  $\text{SO}_4$  groups, and a mode at about 5 meV as the tunnel splitting. We think in fact that the mode at 192 meV is actually a composite of the (coincidentally) nearly degenerate vibration along the bond and the transverse vibration in the  $x$  direction, which we see at 155 and 147 meV, respectively. That these should

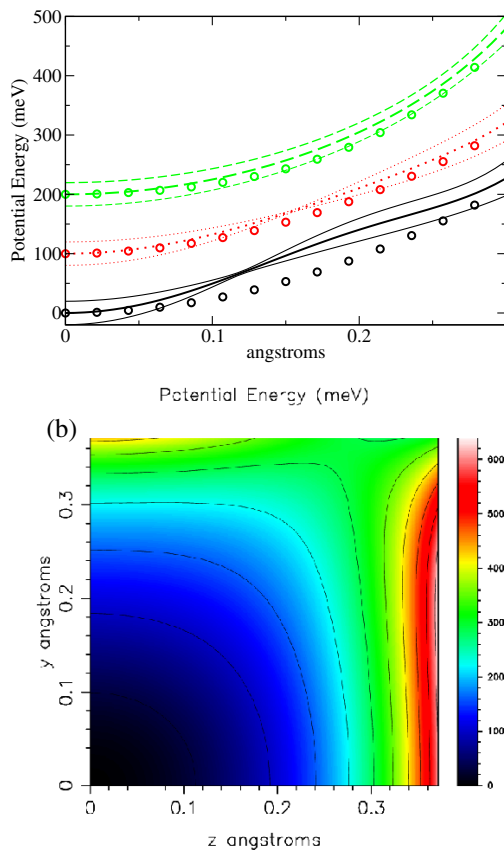


FIG. 2 (color online). BO potential for protons in  $\text{Rb}_3\text{H}(\text{SO}_4)_2$  at 10 K: (a) along the  $x$ -axis (solid line),  $y$ -axis (dotted line), and  $z$ -axis (dashed line), the curves are shifted by 100 meV along the vertical axis for clarity. The errors are shown in dashed lines. The fit to a double Morse potential with parameters shown in the first column of Table II are shown in circles. (b) The potential energy surface in the  $yz$  plane.

be close in frequency can be seen directly from Figs. 2(a) and 3(a). The lack of accuracy of our predicted frequencies is perhaps due to the size of our error bars, which become larger in the region of the excited state energies, where the ground state wave function is small.

This single well potential of the short H bond in the protonated  $\text{Rb}_3\text{H}(\text{SO}_4)_2$  is the reason behind the absence of the low  $T$  antiferroelectric transition that exists in the deuterated systems. Its length is 2.4 Å by our measurements and 2.483 at room temperature [13]. The deuterated H bond, on the other hand, 2.518 Å at 25 K [14] is significantly longer than the protonated one and seems to be, in contrast to the situation in protonated  $\text{Rb}_3\text{H}(\text{SO}_4)_2$ , of the double minimum type.

Double Morse potentials (DMP) have been used to describe O-H-O bonds phenomenologically in a variety of physical systems [2,15–19]. It is of interest to see how close they actually are to the measured potential. We show in Fig. 3(a) the best fitting DMP to our data in the  $yz$  plane. The fit includes our fit of the O-O separation. It can be seen that the fit is semiquantitatively correct. We also tried fitting our momentum distribution measurements with a single Morse potential. This would be appropriate if the symmetric crystal structure were only an average, and individual bonds were actually off center, covalently

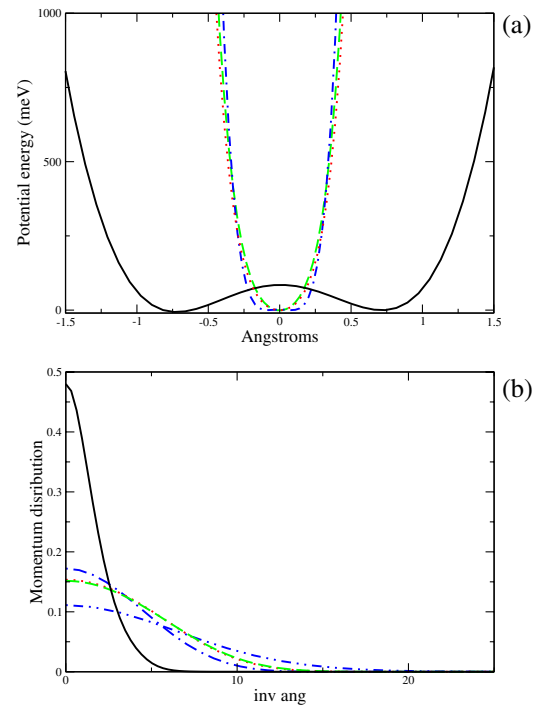


FIG. 3 (color online). Comparing NCS measurements with the double-well potential model of Fillaux and a Morse Potential Model. Fillaux's model is shown in the solid line. The NCS measurements at 10 and 70 K are shown in dotted line and dashed line, respectively. Matsushita and Matsubara's model is shown in dotted-dashed line. (b) The momentum distributions associated with the potentials in (a). The dot-dot dashed line is the fit to a single Morse potential.

TABLE II. Comparison of the measured BO potential, fit with a double Morse potential (DMP) of the form  $U_{\text{dm}}(r) = U(r - z_0) + U(r + z_0)$ , where the single Morse potentials  $U(r) = D\{\exp[-2a(r - r_0)] - 2\exp[-a(r - r_0)]\}$ , with several other DMP models. [Matsushita and Matsubara (MM), Holzapfel (HZ), Mashiyama (MA)].

	This work	MM	HZ	MA
$z_0$ (Å)	$1.2 \pm 0.07$			
$D$ (meV)	$2920 \pm 205$	2150	5337	2200
$a$ (Å <sup>-1</sup> )	$1.96 \pm 0.01$	2.89	$2.8 \pm 0.2$	3.8
$r_0$ (Å)	$0.90 \pm 0.06$	0.95	0.956	1.00

bonded to one or the other of the oxygens. That fit does not work. The models by Holzapfel, Matsushita, *et al.*, Mashiyama, and Borgis *et al.* have momentum distributions of widths 8.2 Å<sup>-1</sup>, 6.6 Å<sup>-1</sup>, 7.5 Å<sup>-1</sup>, and 7.15 Å<sup>-1</sup>, respectively, compared to 4.6 Å<sup>-1</sup> for the harmonic parameter along the bond direction in our measurements. The fact that a symmetric DMP fits the measured potential very well and a single Morse potential localizes the proton far too much is strong indication that the bond is symmetric. The best fit parameters are collected in Table II and compared with those of Holzapfel [15] and Matsushita and Matsubara [2]. The parameters were chosen by Matsushita and Matsubara to reproduce, in a semiempirical way, the structural properties of many OH-O complexes. The parameters in both works represent the average behavior of a wide range of H bonds. They do not necessarily represent an isolated H bond, as in our measurements. A recent study gives very different parameters for a specific system, KDP [19], Table II. The potentials, however, are very similar. We show in Fig. 3(a) the comparison of the potential and momentum distribution obtained by Matsushita and Matsubara when the O-O separation is set to 2.4 Å with no other changes.

Changing the O-O separation in the DMP potential allows for a transition from single to a double-well potential as the O-O separation increases beyond a critical value. The measured critical value for a similar system, K<sub>3</sub>H(SO<sub>4</sub>)<sub>2</sub>, is 2.47 Å [10] compared to 2.51 Å in our DMP fit. Comparing our measurements with *ab-initio* calculations made for isolated hydrogen bonds in aquonium perchlorate [20], we see that a bond length of about 2.4 Å is well into the single well regime. The Path Integral Car-Parinello calculations made by Benoit *et al.* [21] give a critical length of about 2.36 Å. According to this calculation, a bond of a length of 2.4 Å has a very low barrier, several meVs. Such barriers would not be noticeable in our measurements within the experimental error. This is true as well of the small barriers and asymmetry observed in the NMR measurements of Mikacs *et al.* [22] The single well nature of the bond is therefore consistent with all other available evidence.

We have shown here the first measurements of a 3-D BO potential in any system. The measurements can be done on

any symmetric hydrogen bond for which the interaction between the protons in different bonds is negligible. The errors in our measurements are due primarily to counting time limitations on VESUVIO, the one existing machine capable of doing NCS experiments. Its count rate could be improved by a factor of 10 by the addition of more detectors, and another factor of 10 could be achieved by the construction of a similar machine on the Spallation Neutron Source (SNS) or another newer source. We conclude, therefore, that routine measurements of BO potentials in hydrogen-bonded systems to within  $\pm 2$  meV are feasible with existing technology.

The work of G. Reiter and D. Homouz was supported by DOE Grant No. DE-FG02-03ER46078. The authors would like to thank Phil Platzman for his comments and a careful reading of the manuscript and Sossina Haile for useful conversations.

- 
- [1] S. M. Haile, D. A. Boysen, C. R. I. Chisholm, and R. B. Merle, *Nature (London)* **410**, 910 (2001).
  - [2] E. Matsushita and T. Matsubara, *Prog. Theor. Phys.* **67**, 1 (1982).
  - [3] F. Fillaux, A. Lautie, J. Tomkinson, and G. Kearley, *Chem. Phys.* **154**, 135 (1991).
  - [4] G. Reiter and R. Silver, *Phys. Rev. Lett.* **54**, 1047 (1985).
  - [5] K. Gesi, *J. Phys. Soc. Jpn.* **48**, 886 (1979).
  - [6] G. F. Reiter, J. Mayers, and P. Platzman, *Phys. Rev. Lett.* **89**, 135505 (2002).
  - [7] J. Dolinšek, U. Mikac, J. Javoršek, G. Lahajnar, R. Blinc, and L. Kirpichnikova, *Phys. Rev. B* **58**, 8445 (1998).
  - [8] U. Mikac, D. Arčon, B. Zalar, J. Dolinšek, and R. Blinc, *Phys. Rev. B* **59**, 11293 (1999).
  - [9] M. Tachikawa, T. Ishimoto, H. Tokiwa, H. Kasatani, and K. Deguchi, *Ferroelectrics* **268**, 3 (2002).
  - [10] Y. Noda, H. Kasatani, Y. Watanabe, and H. Terauchi, *J. Phys. Soc. Jpn.* **61**, 905 (1992).
  - [11] G. F. Reiter, J. Mayers, and J. Noreland, *Phys. Rev. B* **65**, 104305 (2002).
  - [12] C. Andreani, D. Colognesi, J. Mayers, G. F. Reiter, and R. Senesi, *Adv. Phys.* **54**, 377 (2005).
  - [13] S. Fortier, M. E. Fraser, and R. D. Heyding, *Acta Crystallogr. Sect. C* **41**, 1139 (1985).
  - [14] M. Ichikawa, T. Gustafsson, and I. Olovsson, *Acta Crystallogr. Sect. C* **48**, 603 (1992).
  - [15] W. B. Holzapfel, *J. Chem. Phys.* **56**, 712 (1972).
  - [16] M. C. Lawrence and G. N. Robertson, *Ferroelectrics* **25**, 363 (1980).
  - [17] M. Maćowiak, *Physica B+C (Amsterdam)* **145**, 320 (1987).
  - [18] D. Borgis, G. Tarjus, and H. Azzouz, *J. Chem. Phys.* **97**, 1390 (1992).
  - [19] H. Mashiyama, *J. Phys. Soc. Jpn.* **73**, 3466 (2004).
  - [20] B. S. Hudson and N. Verdal, *Physica B (Amsterdam)* **385-386**, 212 (2006).
  - [21] M. Benoit and D. Marx, *Chem. Phys. Chem.* **6**, 1738 (2005).
  - [22] U. Mikac, B. Zalar, J. Dolinšek, J. Seliger, V. Žagar, O. Plyushch, and R. Blinc, *Phys. Rev. B* **61**, 197 (2000).